Cell Targeting

DOI: 10.1002/anie.201207063

DNA Aptamer-Mediated Cell Targeting**

Xiangling Xiong, Haipeng Liu, Zilong Zhao, Meghan B. Altman, Dalia Lopez-Colon, Chaoyong James Yang, Lung-Ji Chang, Chen Liu, and Weihong Tan**

Cell-based therapy has shown considerable potential in treating diseases such as leukemia and osteoporosis. Certain types of cells, for example, killer lymphocytes that naturally attack cancer cells, are being studied for direct cancer treatment.[1] Other cells, such as mesenchymal stem cells (MSC), can be genetically engineered to produce therapeutics in situ after delivery.[2] However, one important issue in cell-based therapy is the targeted delivery of cells in vivo, which not only improves therapeutic efficacy, but also minimizes side effects. In this regard, several approaches have been studied. A straightforward method involves physical delivery of cells to the site of interest, with the help of proper medical devices.[3] Other targeting strategies, including the use of native cell-homing machinery[4] and expression or coating of cells with targeting ligands, are under intensive study. Carbohydrates,[5] short peptides,[6] and extracellular domains of cell membrane receptors[7] have all been used as targeting moieties.

In recent years, oligonucleotide-based probes, termed aptamers, have been developed with the specificity and affinity required for diagnostic[8] and therapeutic applications.[9] Similar to antibodies, aptamers can specifically recognize a wide range of targets that vary from small molecules to cancer cells.[8,10–12] However, they have additional properties that make them more attractive than antibodies. For example, aptamers are usually smaller, which results in a better ability to penetrate tissue. Furthermore, no immunogenic reactions have thus far been reported for any in vivo experiment with aptamers. Finally, since nucleic acids can be chemically synthesized, aptamers can be readily adapted for modifications to meet different needs.

Our lab has previously developed diacyl phospholipid–DNA conjugates,[13] and herein, we report the use of this lipid–DNA probe to modify cell surfaces for specific cell targeting. We hypothesized that aptamers would induce cellular adhesion upon spontaneous receptor–ligand binding in a manner that mimics the natural process of cell–cell adhesion. We used leukemia cell lines to demonstrate that aptamers anchored on the cell surface could act as targeting ligands that specifically recognize their target cells. Further, we explored the potential of this probe in adoptive cell therapy. Immune-effector cells modified by the probe showed improved affinity, while remaining cytotoxic to target cancer cells. Our method of aptamer-mediated cell targeting is illustrated in Figure 1 a.

To label the cell surface with aptamers, diacyl lipid–DNA aptamer conjugates were synthesized as previously described.[13] A membrane-anchored aptamer can be divided into three distinct segments (Figure 1 a). The first segment is an aptamer sequence selected by a process called cell-SELEX (systematic evolution of ligands by exponential enrichment).[11,12] We have demonstrated in several cancer cell models that aptamers can recognize the molecular differences between target and control cell membranes by preferentially binding to target cells. In this study, two different aptamers, Sgc8, which targets protein tyrosine kinase 7 on CCRF-CEM cell membrane,[11,14] and TD05, which targets the immunoglobulin heavy mu chain on the surface of Ramos cells,[12,15] were used for testing. These aptamers exhibit high affinity ($K_{dSgc8} = 0.8$ nM, $K_{dTD05} = 74$ nM) and excellent selectivity towards their target leukemia cells, as required for mimicking native cell-surface ligand–receptor interactions. Moreover, because multiple aptamers are presented on each cell surface, multivalent interaction with target proteins can greatly improve binding.[16] The second segment is a PEG linker, which allows DNA to extend out from the cell surface, thereby minimizing nonspecific and steric interactions between the cell-surface molecules and the aptamer. As a consequence, the PEG linker facilitates the conformational folding of the aptamer, which is important for aptamer–target binding. The third segment, a synthetic diacyllipid tail with two stearic acids, is conjugated at the 5′ end as the membrane anchor. By its hydrophobic nature, the diacyllipid tail could firmly insert into the cell membrane with excellent efficiency.[13]

[*] X. Xiong, Dr. H. Liu, Dr. M. B. Altman, Dr. D. Lopez-Colon, Prof. L. J. Chang, Prof. C. Liu, Prof. W. Tan
Departments of Chemistry, of Physiology and Functional Genomics, of Molecular Genetics and Microbiology, and of Pathology and Laboratory Medicine, Shands Cancer Center, Center for Research at the Bio/nano Interface, University of Florida
Gainesville, FL 32611-7200 (USA)
E-mail: tan@chem.ufl.edu
Dr. Z. Zhao, Prof. W. Tan
Molecular Science and Biomedicine Laboratory, State Key Laboratory of Chemo/Biosensing and Chemometrics, College of Biology and College of Chemistry and Chemical Engineering, Hunan University, Changsha 410082 (P.R. China)
Prof. C. J. Yang
State Key Laboratory for Physical Chemistry of Solid Surfaces, The Key Laboratory for Chemical Biology of Fujian Province and Department of Chemical Biology, College of Chemistry and Chemical Engineering, Xiamen University, Xiamen 361005 (China)
E-mail: cyyang@xmu.edu.cn

[**] This work is supported by grants awarded by the National Institutes of Health (GM066137, GM079359 and CA133086), by the National Key Scientific Program of China (2011CB911000), the China National Instrumentation Program (2011YQ03012412), and the Foundation for Innovative Research Groups of NSFC (21221003).
Supporting information for this article is available on the WWW under http://dx.doi.org/10.1002/anie.201207063.

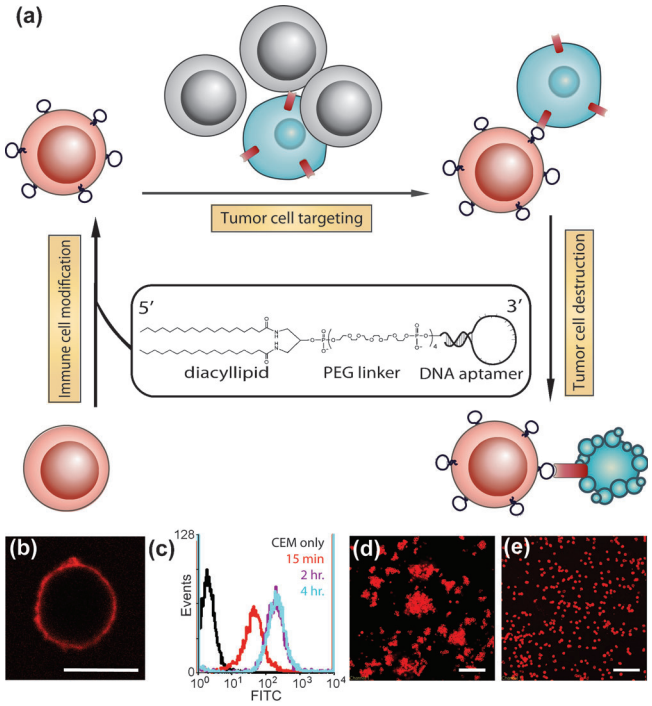

Figure 1. Modification of cell membranes with aptamers. a) Illustration of targeting cancer cells (blue) with aptamer-modified immune cells (red). After incubating with lipo–aptamer probes (shown in expansion), immune cells recognize and kill cancer cells in the cell mixture. b) Confocal microscope image of lipo-Lib-TMR-treated CEM cells. Red fluorescent probes were found only on the cell surface. Scale bar: 10 μm. c) CEM cells were treated with lipo-Lib-FITC for different time intervals in cell culture medium. The maximum insertion was reached at 2 h. d) Ramos cells spontaneously aggregate after treatment with lipo-TD05-TMR. Scale bar: 100 μm. e) Control experiments showed no assembly when Ramos cells were treated with lipo-lib-TMR. Scale bar: 100 μm.

To demonstrate lipid insertion, a fluorescent dye molecule (TAMRA) was conjugated to the 3′ end of the oligonucleotides. After incubation with cells, the labeled lipid–DNA probes were detected on the cell membrane by confocal microscopy (Figure 1 b). Aptamer density on the cell surface can be easily controlled by varying the incubation time or initial DNA probe concentration. As shown by flow cytometry, a higher initial concentration generally resulted in more aptamers anchored on the cell surface, and after 1 μM concentration, the increment of probe concentration did not improve insertion much for CEM cells (Supporting Information, Figure S1 a). Also, lipid insertion could be observed within 15 min and reached equilibrium after two hours in cell culture medium (Figure 1 c). Similarly, immune effector cells such as natural killer (NK) cells and T cells can be modified with lipo–DNA probes as well (Figure S1 b,c).

To test whether the aptamers could fold properly to recognize their targets after anchoring on the cell membrane, we first designed a homotypic cell targeting experiment. We expected that cells modified with their targeting aptamer would form a cell-aptamer-cell assembly. As shown in Figure 1 d, the TD05-treated Ramos cells spontaneously formed sequence-specific aggregates. In control experiments where Ramos cells were incubated with a random sequence (lipo-Lib-TMR), no aggregates were observed (Figure 1 e). Similar homotypic assemblies were observed for CEM cells modified with Lipo-Sgc8-TMR (Figure S2). The above experiments supported our hypothesis that membrane-anchored aptamers could induce cellular adhesion in a defined target-specific fashion.

To further demonstrate aptamer specificity, we designed experiments to show different types of cell assemblies. Ramos cells were first treated with lipo-Sgc8-TMR (fluorescent), and mixed with unmodified CEM cells (nonfluorescent) at a 1:10 ratio. Cell aggregates with a flower-like structure were observed (Figure 2 a and b). Each cluster contained two types of cells: surface-modified fluorescent cells and non-fluorescent target cells. Heterotypic cell adhesions were also observed between CEM and Ramos cells using lipo-TD05-TMR (Figure S3). The generality of this assembly strategy was demonstrated by crosslinking CEM/Ramos with other cell lines, such as Jurkat and K562, using similar procedures (Figures S4 and S5).

Controlled cell aggregation could also be realized in mixed cell populations. For example, K562 cells were labeled with lipo-Sgc8-TMR or lipo-TD05-TMR, and then a mixture of CEM (nonfluorescent) and Ramos cells (CellTracker Green-labeled) was added. Depending on which aptamer was used, K562 specifically recognized CEM or Ramos in the mixture (Figure 2 c and d), and no mismatched cell aggregates were observed. This indicated that aptamers anchored on the cell membranes were still very specific and could therefore be applied in a biological system.

Finally, we quantified the cell aggregation using flow cytometry. As presented in Figure 2 e, 40–95 % CEM cells formed aggregates with Ramos cells when modified with TD05, compared with less than 5 % aggregate formation in DNA-library-modified CEM cells (Table S1). The percentage of aggregation can be controlled by the aptamer concentration and the ratio of modified cells to target cells. An increase in probe concentration up to 1 μM can significantly increase the aggregation percentage. From 1 μM to 2 and up to 5 μM, the increase is small because 1 μM modification was sufficient to cause 80–90 % cell aggregation, and the number of lipo–DNA on the cell surface was close to each other (Figure S1 a). On the other hand, since an increased number of target cells can increase the chance of interaction, more aggregates were formed when an excess of Ramos cells was used.

To further confirm that the cell assembly was induced by DNA aptamers anchored on cell surfaces, the aggregates were treated with a nuclease and a protease that can destroy either aptamers or target proteins, respectively. First, CEM cells modified with lipo-Lib-TMR or lipo-TD05-TMR probes were mixed with 5 equivalents of Ramos cells (CellTracker Green-labeled). Images taken immediately after mixing showed that most CEM and Ramos cells remained apart with only a few small aggregates (Figure S7). After 20 min incubation, as expected, almost all of the TD05 aptamer-modified CEM cells were surrounded by Ramos cells, resulting in a yellow (combination of red and green) fluorescent signal (Figure 2 f, and Figure S8 b), whereas library-labeled CEM cells did not form any aggregates with Ramos cells (Figure 2 h and Fig-

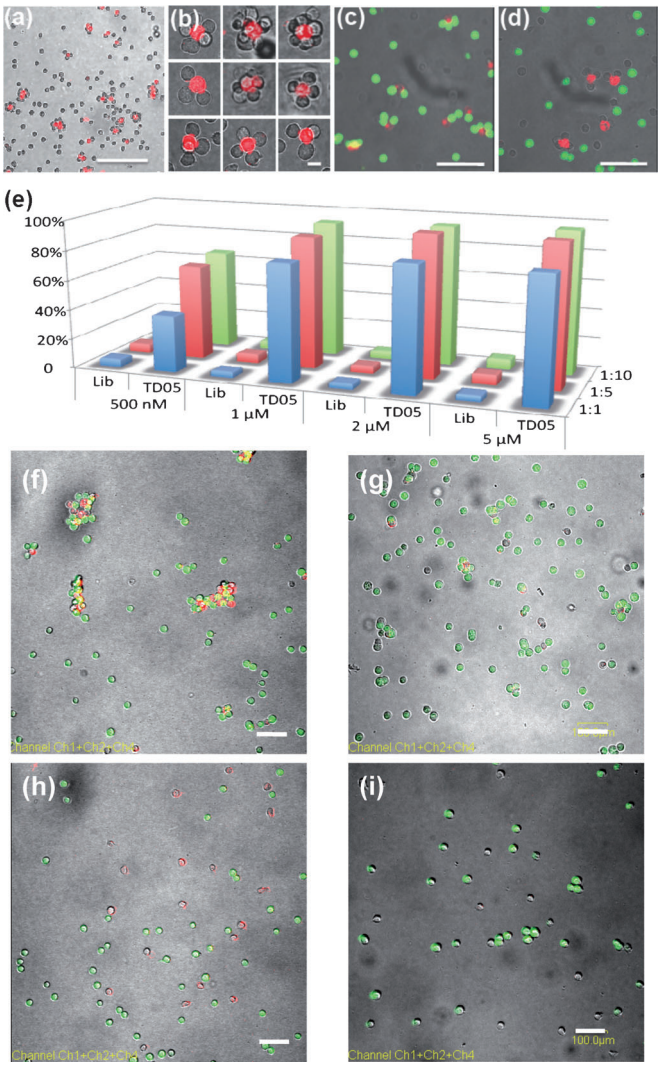

Figure 2. Aptamer-directed assembly and disassembly of cell aggregates, and quantitative analysis of aggregation. a) A 1:10 mixture of lipo-sgc8-TMR-modified Ramos and CEM cells. Scale bar: 100 μm. b) Discrete cell clusters at higher magnification. Scale bar: 10 μm. c) Confocal micrograph of selective cell assembly. Lipo-TD05-TMR-modified K562 cells (red fluorescence) were incubated with CellTracker Green-labeled Ramos cells (green fluorescence) and unlabeled CEM cells. No mismatched cell assembly (K562 and CEM cells or Ramos and CEM cells) was observed. Scale bar: 50 μm. d) Confocal micrograph of selective cell assembly of lipo-Sgc8-TMR-modified K562 cells (red fluorescence) and unlabeled CEM cells. e) Aggregation percentage of CEM cells in different sample sets. Ratios of CEM cells to Ramos cells are represented by blue (1:1), red (1:5) and green (1:10) bars. f) A 1:5 mixture of lipo-TD05-TMR-modified CEM cells (red) and Ramos cells (green) after 20 min incubation. CEM and Ramos cells formed aggregates. Scale bar: 100 μm. g) Mixture of Lipo-TD05-TMR-modified CEM (red) cells and Ramos (green) cells from (f) treated with DNase I. Scale bar: 100 μm. h) A 1:5 mixture of lipo-Lib-TMR-modified CEM (red) cells and Ramos (green) cells after 25 min incubation. CEM and Ramos cells remained apart. Scale bar: 100 μm. i) Mixture of Lipo-Lib-TMR-modified CEM (red) cells and Ramos (green) cells from (h) treated with DNase I. Scale bar: 100 μm.

ure S8a). Finally, these cell aggregates were treated with deoxyribonuclease I, which can cleave single- and double-stranded DNA. As shown in Figure 2g,i, after treatment, the red fluorescent signal on CEM cells disappeared because the TMR dye molecule had been cleaved from the cell surface. Moreover, fewer aggregates can be seen in Figure 2g than in Figure 2f, which indicates that the aggregation caused by aptamer–target recognition had been disrupted by removal of DNA aptamers from the modified cell surfaces. It is noteworthy that some small aggregates remained, as shown in Figure 2g, and that the interface between these two cells remained yellow. One possible reason is that the binding of these two cells was so tight that DNase was prevented from interacting with the aptamers by steric hindrance; consequently, the aggregates remained intact. We also treated cellular aggregates with proteinase K, a protein known to digest the target surface proteins of Ramos cells,[15] which resulted in the disassembly of aggregated cells and the uniform dispersion of individual cells (Figure S9).

As delivered cells are intended for therapy, modification of the cell surface should not affect cellular functions. The components of the probe, including oligonucleotides, PEG polymers, and diacyl lipids, are not known to be cytotoxic. To test whether the insertion had any toxic effect on cells, cell necrosis and apoptosis were tested after modification, and minimal cell death was observed (Figure S10a). The proliferation rate was monitored using a cell proliferation assay, and no significant change was observed in any cell lines with 1 μM modification (Figure S10b). These results suggested that the probe itself is not cytotoxic at 1 μM concentration.

To further investigate the cellular effect of the lipid–DNA probe on immune effector cells, we used NK cells, a type of killer lymphocyte, as a model. NK cells recognize cells independent of major histocompatibility complex (MHC), and they kill cells that do not express MHC by releasing granule proteins.[17] K562, a type of chronic myelogenous leukemia cell line, is often used as a target for in vitro NK cell assays.[18] The aptamer used in this study was KK1B10, an aptamer that specifically recognizes K562 cells.[19] In the binding assay (Figure 3a), unmodified and library-modified NK groups showed a higher background binding (about 40%) than previously demonstrated CEM-Ramos binding assays. This is because NK cells spontaneously recognize K562 cells. Aptamer modification of NK cells targeted 60% of the K562 cells, which improved NK cell targeting efficiency by 50% compared with unmodified and library-modified NK cells.

To determine if NK cells modified with the KK1B10 aptamer would affect their killing functions, we set up a NK cytolytic assay, as previously reported.[20] Compared with unmodified NK cells, control library-modified NK cells showed the same killing effect on K562 cells (around 21%; Figure 3b), which indicates that lipo–DNA would not interfere with the cell-mediated cytotoxicity. Moreover, NK cells modified with KK1B10 aptamer killed about 30% of K562 cells, which was 50% more than unmodified NK cells. The incremental killing efficiency correlated well with targeting efficiency. The virtue of adding aptamers as extra targeting ligands was revealed in the presence of excess non-target cells. In this experiment, K562 cells were first mixed with four equivalents of non-target Ramos cells and then incubated with NK cells. Within the same amount of time, NK cells

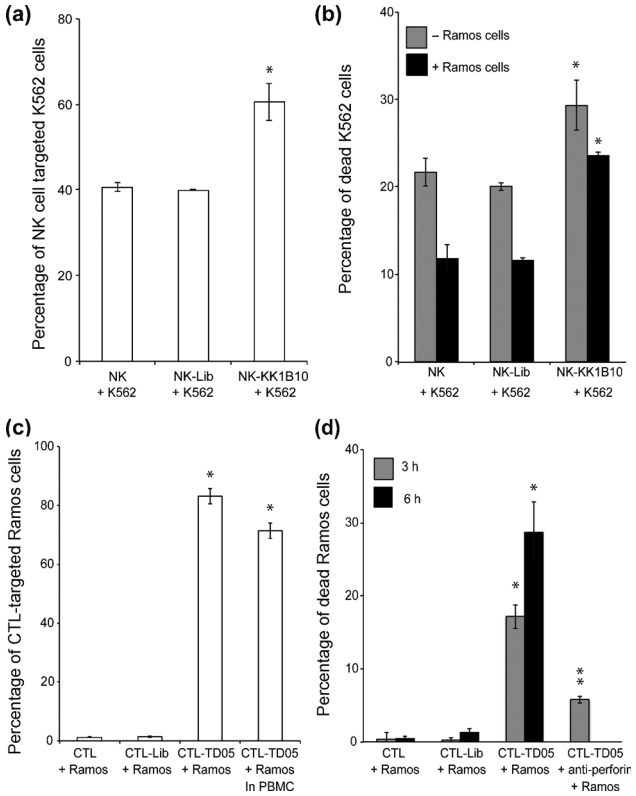

Figure 3. Aptamer-assisted immune effector cell targeting and killing of leukemia cells a) NK–K562 cell binding assay. NK cells recognize K562 cells spontaneously; however, aptamer modification improved targeting by 50%. b) NK-K562 cell killing assay. Aptamer-modified NK cells killed K562 cells more effectively, especially in the presence of background cells (Ramos). c) CTL–Ramos cell binding assay. Without presenting the specific MHC I peptide on Ramos cell surfaces, CTL cannot recognize Ramos cells. On the other hand, aptamer-modified CTL recognized 80% of Ramos cells. d) CTL–Ramos cell killing assay. Assisted by membrane-anchored aptamers, CTL targeted and killed Ramos cells through cell-mediated immunity. CTL-mediated cytotoxicity was confirmed by blocking the perforin/granzyme pathway with an antibody. Values are means with SD ($n=3$). The single asterisk indicates a significant difference between aptamer-modified and unmodified or Lib-modified groups determined by the one-tailed t-test at $P<0.01$. The double asterisks indicate a significant difference between aptamer-modified and anti-Perforin treated groups determined by the one-tailed t-test at $P<0.01$.

killed fewer K562 cells, but the decrease was considerably smaller in the aptamer-modified group, thus suggesting that aptamer modification can improve cell targeting without affecting immune effector function (Figure 3b).

These results suggested the feasibility of a novel T-cell killing model, in which the specific cytotoxicity was controlled by membrane-anchored aptamers. A primary immortalized cytomegalovirus (CMV)-specific CD8+ cytotoxic T lymphocyte (CTL) clone (HLA A0201) preactivated with 12-myristate 13-acetate (PMA) and ionomycin was used as the immune effector cell type. The target cells were Ramos cells, a B-cell Burkitt's lymphoma cell line. Ionomycin synergizes with PMA to activate protein kinase C, resulting in perforin-granule release from CTL.[21] The perforin/granzyme cell death pathway requires direct contact between effector and target cells.[22] Therefore, without a CMV-specific peptide–MHC I complex on Ramos cell surfaces, the CMV-specific CTL cannot recognize Ramos cells, thus resulting in only a background cytotoxic effect towards Ramos. However, when assisted by surface-anchored TD05 aptamers, the modified CTL have increased affinity toward target Ramos cells, thereby facilitating and prolonging interactions between effector and target cells. Thus, enhanced killing of Ramos cells should be observed.

To test this, we first performed a binding assay to study the binding between CTL and Ramos cells. Figure 3c shows that CTL did not recognize Ramos cells naturally, unless they were modified with the targeting aptamers. Within 20 min, 80% of Ramos cells were targeted by CTL in the cell culture. To test the targeting effectiveness under more biologically relevant conditions, Ramos cells were spiked into peripheral blood mononuclear cells (PBMC) and then incubated with the CTL. The targeting effectiveness was slightly influenced by the spiked PBMC, resulting in targeting 70% of Ramos cells.

We then designed the CTL-Ramos cell-killing assay in a manner similar to the previously described NK-K562 cell-killing assay (Figure S11). As shown in Figure 3d, about 15% and 30% of Ramos cells were dead in the aptamer-modified CTL group in 3 h and 6 h, respectively, whereas <5% dead Ramos cells were found in Lib-modified or unmodified CTL groups. To confirm that Ramos cell death was caused by CTL, an anti-perforin antibody that blocks the perforin/granzyme pathway[23] was added to the aptamer-modified group. The percentage of dead Ramos cells was greatly reduced, from 15% to 5%. This aptamer-modified CTL-killing assay demonstrated that aptamers could redirect specific CTL killing towards the desired target cells, which shed light on potential applications of the lipo–aptamer probes in adoptive cancer immunotherapy. It is noteworthy that aptamers endowed CTL with new targeting specificity, and that the recognition was independent of MHC, which is a major limitation of CTL therapy. An in vivo model to study the trafficking of aptamer-modified cells and immune effector killing is under investigation in our group.

In conclusion, we have successfully engineered a novel targeting ligand on cell membranes for specific cell targeting. We have demonstrated that the noncovalent modification is simple, yet effective, with no short-term effect on modified cells. The selective assembly of multiple types of cells by aptamer–protein recognition is rapid and target-specific. Immune effector cells modified with aptamers can recognize leukemia cells through MHC nonrestricted structures, thus leading to elevated cancer cell targeting and killing. Using a CMV-specific CD8+ CTL clone as immune effector cells and Ramos cells as target cells, we have demonstrated, for the first time, a redirected cell killing by T cells, where the specificity was controlled by aptamers. Further study will focus on the metabolism of the synthetic lipid and in vivo cell trafficking. We believe that the diversity of aptamer targets and the facile nature of the modification make this strategy attractive in cell-based delivery and therapy.

Received: August 31, 2012
Published online: December 11, 2012

Keywords: aptamers · cell modification · cell recognition · cell-based immunotherapy · DNA

[1] P. van der Bruggen, C. Traversari, P. Chomez, C. Lurquin, E. De Plaen, B. Van den Eynde, A. Knuth, T. Boon, *J. Immunol.* **2007**, *178*, 2617 – 2621; Y. Kawakami, S. Eliyahu, C. H. Delgado, P. F. Robbins, K. Sakaguchi, E. Appella, J. R. Yannelli, G. J. Adema, T. Miki, S. A. Rosenberg, *Proc. Natl. Acad. Sci. USA* **1994**, *91*, 6458 – 6462; P. A. Albertsson, P. H. Basse, M. Hokland, R. H. Goldfarb, J. F. Nagelkerke, U. Nannmark, P. J. K. Kuppen, *Trends Immunol.* **2003**, *24*, 603 – 609.

[2] C. Conrad, R. Gupta, H. Mohan, H. Niess, C. J. Bruns, R. Kopp, I. von Luettichau, M. Guba, C. Heeschen, K.-W. Jauch, R. Huss, P. J. Nelson, *Curr. Gene Ther.* **2007**, *7*, 249 – 260; J. Reiser, X. Y. Zhang, C. S. Hemenway, D. Mondal, L. Pradhan, V. F. La Russa, *Expert Opin. Biol. Ther.* **2005**, *5*, 1571 – 1584; L. Elzaouk, K. Moelling, J. Pavlovic, *Exp. Dermatol.* **2006**, *15*, 865 – 874.

[3] A. M. Parr, I. Kulbatski, C. H. Tator, *J. Neurotrauma* **2007**, *24*, 835 – 845; K.-K. Poh, E. Sperry, R. G. Young, T. Freyman, K. G. Barringhaus, C. A. Thompson, *Int. J. Cardiol.* **2007**, *117*, 360 – 364.

[4] C. G. Millán, M. L. S. Marinero, A. Z. Castaneda, J. M. Lanao, *J. Controlled Release* **2004**, *95*, 27 – 49; R. A. Freitas, *J. Nanosci. Nanotechnol.* **2006**, *6*, 2769 – 2775.

[5] C. Foxall, S. R. Watson, D. Dowbenko, C. Fennie, L. A. Lasky, M. Kiso, A. Hasegawa, D. Asa, B. K. Brandley, *J. Cell Biol.* **1992**, *117*, 895 – 902; D. Sarkar, J. A. Spencer, J. A. Phillips, W. A. Zhao, S. Schafer, D. P. Spelke, L. J. Mortensen, J. P. Ruiz, P. K. Vemula, R. Sridharan, S. Kumar, R. Karnik, C. P. Lin, J. M. Karp, *Blood* **2011**, *118*, e184 – e191.

[6] O. Mandelboim, E. Vadai, M. Fridkin, A. Katzhillel, M. Feldman, G. Berke, L. Eisenbach, *Nat. Med.* **1995**, *1*, 1179 – 1183; F. O. Nestle, S. Alijagic, M. Gilliet, Y. Sun, S. Grabbe, R. Dummer, G. Burg, D. Schadendorf, *Nat. Med.* **1998**, *4*, 328 – 332.

[7] B. Jena, G. Dotti, L. J. N. Cooper, *Blood* **2010**, *116*, 1035 – 1044; D. L. Porter, B. L. Levine, M. Kalos, A. Bagg, C. H. June, *N. Engl. J. Med.* **2011**, *365*, 725 – 733.

[8] A. D. Ellington, J. W. Szostak, *Nature* **1990**, *346*, 818 – 822; C. Tuerk, L. Gold, *Science* **1990**, *249*, 505 – 510.

[9] A. D. Keefe, S. Pai, A. Ellington, *Nat. Rev. Drug Discovery* **2010**, *9*, 537 – 550.

[10] M. Rajendran, A. D. Ellington, *Comb. Chem. High Throughput Screening* **2002**, *5*, 263 – 270; M. Rajendran, A. D. Ellington, *Anal. Bioanal. Chem.* **2008**, *390*, 1067 – 1075; A. Geiger, P. Burgstaller, H. von der Eltz, A. Roeder, M. Famulok, *Nucleic Acids Res.* **1996**, *24*, 1029 – 1036.

[11] D. Shangguan, Y. Li, Z. W. Tang, Z. H. C. Cao, H. W. Chen, P. Mallikaratchy, K. Sefah, C. Y. J. Yang, W. H. Tan, *Proc. Natl. Acad. Sci. USA* **2006**, *103*, 11838 – 11843.

[12] Z. W. Tang, D. Shangguan, K. M. Wang, H. Shi, K. Sefah, P. Mallikratchy, H. W. Chen, Y. Li, W. H. Tan, *Anal. Chem.* **2007**, *79*, 4900 – 4907.

[13] H. P. Liu, Z. Zhu, H. Z. Kang, Y. R. Wu, K. Sefan, W. H. Tan, *Chem. Eur. J.* **2010**, *16*, 3791 – 3797.

[14] D. Shangguan, Z. Cao, L. Meng, P. Mallikaratchy, K. Sefah, H. Wang, Y. Li, W. Tan, *J. Proteome Res.* **2008**, *7*, 2133 – 2139.

[15] P. Mallikaratchy, Z. W. Tang, S. Kwame, L. Meng, D. H. Shangguan, W. H. Tan, *Mol. Cell. Proteomics* **2007**, *6*, 2230 – 2238.

[16] Y.-F. Huang, H.-T. Chang, W. Tan, *Anal. Chem.* **2008**, *80*, 567 – 572.

[17] H. G. Ljunggren, K. Karre, *Immunol. Today* **1990**, *11*, 237 – 244.

[18] J. R. Ortaldo, R. K. Oldham, G. C. Cannon, R. B. Herberman, *J. Natl. Cancer Inst.* **1977**, *59*, 77 – 82.

[19] K. Sefah, Z. W. Tang, D. H. Shangguan, H. Chen, D. Lopez-Colon, Y. Li, P. Parekh, J. Martin, L. Meng, J. A. Phillips, Y. M. Kim, W. H. Tan, *Leukemia* **2009**, *23*, 235 – 244.

[20] M. Marcusson-Ståhl, K. Cederbrant, *Toxicology* **2003**, *193*, 269 – 279.

[21] T. Chatila, L. Silverman, R. Miller, R. Geha, *J. Immunol.* **1989**, *143*, 1283 – 1289.

[22] J. A. Trapani, M. J. Smyth, *Nat. Rev. Immunol.* **2002**, *2*, 735 – 747.

[23] H. G. Otten, W. G. J. van Ginkel, A. Hagenbeek, E. J. Petersen, *Leukemia* **2004**, *18*, 1401 – 1405.

